Quantum Discrimination of Noisy Photon-Added Coherent States

Stefano Guerrini, *Student Member, IEEE*, Moe Z. Win, *Fellow, IEEE*, Marco Chiani, *Fellow, IEEE*, and Andrea Conti, *Senior Member, IEEE*

***Abstract*—Quantum state discrimination (QSD) is a key enabler in quantum sensing and networking, for which we envision the utility of non-coherent quantum states such as photon-added coherent states (PACSs). This paper addresses the problem of discriminating between two noisy PACSs. First, we provide representation of PACSs affected by thermal noise during state preparation in terms of Fock basis and quasi-probability distributions. Then, we demonstrate that the use of PACSs instead of coherent states can significantly reduce the error probability in QSD. Finally, we quantify the effects of phase diffusion and photon loss on QSD performance. The findings of this paper reveal the utility of PACSs in several applications involving QSD.**

***Index Terms*—Quantum state discrimination, photon-added coherent state, quantum noise, quantum communications.**

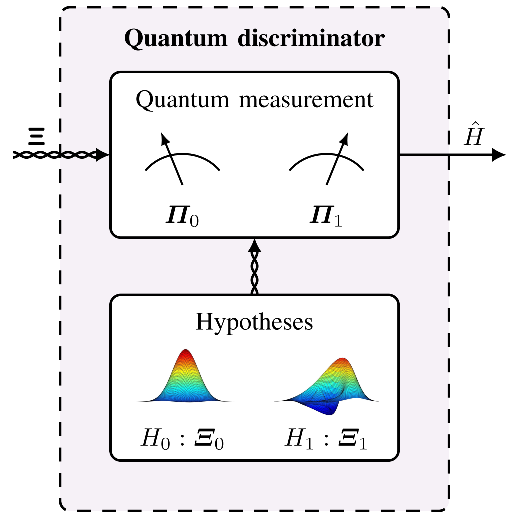

Fig. 1. Illustration of binary QSD with PACSs: hypotheses are described by the Wigner functions corresponding to the quantum states.

I. INTRODUCTION

QUANTUM STATE DISCRIMINATION (QSD) addresses the problem of identifying an unknown state among a set of quantum states [1]–[3]. QSD enables several applications including quantum communications [4]–[6], quantum sensing [7]–[9], quantum illumination [10]–[12], quantum cryptography [13]–[15], quantum networks [16]–[18], and quantum computing [19]–[21]. The discrimination error probability (DEP) depends on the set of quantum states and the measurement used to discriminate among them. Determining the DEP and identifying the quantum measurement that minimizes the DEP are difficult tasks, especially for states prepared in the presence of thermal noise (hereafter referred to as noisy states).

Understanding how the choice of quantum states impacts the discrimination performance plays an important role in QSD applications. In particular, continuous-variable quantum states have been considered in quantum optics as they supply a quantum description of the electromagnetic field and can be efficiently prepared, manipulated, and measured [22]–[28]. Previous works on continuous-variable QSD have devoted particular attention to the analysis of discrimination between coherent states [29]–[34], largely motivated by the success of the Glauber theory [35]–[38].

In contrast, QSD with non-coherent states has received less attention except for attempts made on the use of squeezed states [39]–[41] and number states [42]–[44]. Photon-added coherent states (PACSs) are another important class of non-coherent quantum states that can be generated in a laboratory [45]–[47]. PACSs have been considered for quantum communications [48] and quantum cryptography [49] but a characterization of QSD with PACSs is still missing. Determining the effects of thermal noise on QSD requires a mathematical representation of the quantum states. The Wigner function of noisy PACSs was given in [50]–[52]. However, a complete representation of noisy PACSs is still missing.

The fundamental questions related to QSD with non-coherent states are: (i) which class of quantum states can be used to minimize the DEP; and (ii) how does this class of states perform when affected by thermal noise? The answers

Manuscript received February 15, 2020; revised July 10, 2020; accepted July 21, 2020. Date of publication July 30, 2020; date of current version September 22, 2020. The fundamental research described in this paper was supported in part by the Italian MIUR under the Program Dipartimenti di Eccellenza (2018–2022), in part by the Office of Naval Research under Grant N62909-18-1-2017 and Grant N00014-19-1-2724, and in part by the MIT Institute for Soldier Nanotechnologies. *(Corresponding author: Andrea Conti.)*

Stefano Guerrini and Andrea Conti are with the Department of Engineering and CNIT, University of Ferrara, 44122 Ferrara, Italy (e-mail: stefano.guerrini@unife.it; a.conti@ieee.org).

Moe Z. Win is with the Laboratory for Information and Decision Systems, Massachusetts Institute of Technology, Cambridge, MA 02139 USA (e-mail: moewin@mit.edu).

Marco Chiani is with the Department of Electrical, Electronic, and Information Engineering "Guglielmo Marconi" and CNIT, University of Bologna, 40136 Bologna, Italy (e-mail: marco.chiani@unibo.it).

Digital Object Identifier 10.1109/JSAIT.2020.3012944

to these questions provide insights into the utility of non-coherent states for QSD. The use of non-coherent states can be envisioned for many applications relying on QSD. In particular, PACSs can provide significant benefits to QSD and pave the way for innovative applications in quantum sensing and networking. The goal of this paper is to establish the use of PACSs to improve QSD.

This paper characterizes the QSD with PACSs (see Fig. 1). In particular, the key contributions of the paper can be summarized as follows:

- representation of noisy PACSs in terms of Fock basis, Wigner W-function, Glauber–Sudarshan P-function, and Husimi–Kano Q-function;
- characterization of QSD with noisy PACSs in terms of DEP for optimal/suboptimal quantum measurements; and
- quantification of decoherence effects, such as phase diffusion and photon loss, on QSD performance.

The remainder of the paper is organized as follows. Section II characterizes QSD with noiseless PACSs. Section III provides a mathematical representation of noisy PACSs. Section IV analyzes the discrimination of noisy PACSs. Section V quantifies the effects of phase and photon losses on the QSD. Final remarks are given in Section VI.

Notation: Random variables are displayed in sans serif, upright fonts; their realizations in serif, italic fonts. Operators are denoted by uppercase letters. For example, a random variable and its realization are denoted by x and x; a random operator and its realization are denoted by X and $\boldsymbol{X}$, respectively. The sets of complex numbers and of positive integer numbers are denoted by $\mathbb{C}$ and $\mathbb{N}$, respectively. For $z \in \mathbb{C}$: $|z|$ and $\arg(z)$ denote the absolute value and the phase, respectively; z_r and z_i denote the real part and the imaginary part, respectively; z^* is the complex conjugate; and $\imath = \sqrt{-1}$. The trace and the adjoint of an operator are denoted by $\mathrm{tr}\{\cdot\}$ and $(\cdot)^\dagger$, respectively. The annihilation, the creation, and the identity operators are denoted by $\boldsymbol{A}$, $\boldsymbol{A}^\dagger$, and $\boldsymbol{I}$, respectively. The trace norm of an operator is represented by $\|\cdot\|_1$. The displacement operator with parameter $\mu \in \mathbb{C}$ is $\boldsymbol{D}_\mu = \exp\{\mu \boldsymbol{A}^\dagger - \mu^* \boldsymbol{A}\}$. The rotation operator with parameter $\phi \in \mathbb{R}$ is $\boldsymbol{R}_\phi = \exp\{-\imath\phi \boldsymbol{A}^\dagger \boldsymbol{A}\}$. The Kronecker delta function, the discrete delta function, and the generalized delta function are denoted by $\delta_{n,m}$, δ_n, and $\delta(\cdot)$, respectively.

II. Preliminaries

This section briefly reviews binary QSD, and the discrimination of noiseless PACSs.

A. Binary Quantum State Discrimination

Binary QSD aims to identify an unknown state among a set of two quantum states. This requires the design of a binary positive operator-valued measure (POVM)[1] to distinguish between two quantum states described by the density operators $\boldsymbol{\Xi}_0$ and $\boldsymbol{\Xi}_1$. This can be formulated as an hypothesis testing problem [1], as depicted in Fig. 1. In particular, let $\mathsf{\Xi}$ be the unknown quantum state,[2] then the binary hypotheses are described by

$$\begin{aligned} H_0 &: \mathsf{\Xi} = \boldsymbol{\Xi}_0 \\ H_1 &: \mathsf{\Xi} = \boldsymbol{\Xi}_1. \end{aligned} \tag{1}$$

The quantum states $\boldsymbol{\Xi}_0$ and $\boldsymbol{\Xi}_1$ have prior probability p_0 and p_1, respectively. Under these premises, the DEP is

$$P_\mathrm{e} = p_0 \mathrm{tr}\{\boldsymbol{\Xi}_0 \boldsymbol{\Pi}_1\} + p_1 \mathrm{tr}\{\boldsymbol{\Xi}_1 \boldsymbol{\Pi}_0\}. \tag{2}$$

The problem of finding an optimal POVM that minimizes the DEP has been extensively studied in [1]. In the binary case, the minimum DEP (MDEP) is given by the well known Helstrom bound

$$\breve{P}_\mathrm{e} = \frac{1}{2}\big(1 - \|p_1 \boldsymbol{\Xi}_1 - p_0 \boldsymbol{\Xi}_0\|_1\big). \tag{3}$$

The optimal POVM that achieves the Helstrom bound is given by the following expressions

$$\boldsymbol{\Pi}_0 = \sum_{\substack{i \\ \lambda_i < 0}} |\lambda_i\rangle\langle\lambda_i| \tag{4a}$$

$$\boldsymbol{\Pi}_1 = 1 - \boldsymbol{\Pi}_0 = \sum_{\substack{i \\ \lambda_i \geq 0}} |\lambda_i\rangle\langle\lambda_i| \tag{4b}$$

where $|\lambda_i\rangle$ is the eigenvector of $p_1\boldsymbol{\Xi}_1 - p_0\boldsymbol{\Xi}_0$ associated with the eigenvalue λ_i. For pure states, i.e., $\boldsymbol{\Xi}_0 = |\psi_0\rangle\langle\psi_0|$ and $\boldsymbol{\Xi}_1 = |\psi_1\rangle\langle\psi_1|$, the MDEP is given by

$$\breve{P}_\mathrm{e} = \frac{1}{2}\Big(1 - \sqrt{1 - 4p_0p_1|\langle\psi_0|\psi_1\rangle|^2}\Big). \tag{5}$$

Note that, in this case, the MDEP is zero when the two states are orthogonal, i.e., $\langle\psi_0|\psi_1\rangle = 0$. In the case of mixed states, the MDEP is zero when the density operators $\boldsymbol{\Xi}_0$ and $\boldsymbol{\Xi}_1$ have support on orthogonal subspaces [53].

B. Discrimination of Noiseless Photon-Added Coherent States

PACSs were first introduced in [45] and successfully generated in a laboratory [46], [47]. A PACS is defined as follows

$$|\mu^{(k)}\rangle = \frac{(\boldsymbol{A}^\dagger)^k|\mu\rangle}{\sqrt{\langle\mu|\boldsymbol{A}^k(\boldsymbol{A}^\dagger)^k|\mu\rangle}} \tag{6}$$

where $|\mu\rangle$ is a coherent state of amplitude $\mu \in \mathbb{C}$ and $k \in \mathbb{N}$ represents the number of addition operations.

Consider now the discrimination of PACS in a noiseless scenario, i.e., the states associated with the hypotheses in (1) are given by $\boldsymbol{\Xi}_0 = |\xi^{(h)}\rangle\langle\xi^{(h)}|$ and $\boldsymbol{\Xi}_1 = |\mu^{(k)}\rangle\langle\mu^{(k)}|$. Since the states are pure, the MDEP is determined by (5) with $|\psi_0\rangle = |\xi^{(h)}\rangle$ and $|\psi_1\rangle = |\mu^{(k)}\rangle$, and its dependence on the quantum states is manifested by the following Lemma.

[1]A binary POVM is a set with two positive operators $\{\boldsymbol{\Pi}_0, \boldsymbol{\Pi}_1\}$ such that $\boldsymbol{\Pi}_0 + \boldsymbol{\Pi}_1 = \boldsymbol{I}$.

[2]In the following, the term "quantum state" and corresponding "density operator" will be used interchangeably.

Lemma 1: Consider two PACSs $|\xi^{(h)}\rangle$ and $|\mu^{(k)}\rangle$ according to (6). Without loss of generality, let $h \leq k$. It is

$$\langle\xi^{(h)}|\mu^{(k)}\rangle = \frac{(\xi^*)^{k-h} L_h^{k-h}(-\mu\xi^*)\, e^{-\frac{1}{2}(|\mu|^2+|\xi|^2-2\mu\xi^*)}}{\sqrt{\frac{k!}{h!} L_k(-|\mu|^2) L_h(-|\xi|^2)}} \quad (7)$$

where $L_h(x)$ is the Laguerre polynomial of degree h and $L_h^{k-h}(x)$ is the generalized Laguerre polynomial of degree h with parameter $k-h$ [54].

Proof: See Appendix A. □

The MDEP is found by using (7) in (5). Note that the scalar product between the two states, and thus the MDEP, is zero if one of the following orthogonality conditions holds

$$\text{(i)}\quad \xi = 0 \text{ and } h \neq k \quad (8a)$$

$$\text{(ii)}\quad L_h^{k-h}(-\mu\xi^*) = 0. \quad (8b)$$

The orthogonality condition (8a) is of particular interest because $|\xi^{(h)}\rangle$ with $\xi = 0$ corresponds to the Fock state $|h\rangle$. In particular, this is related to the fact that the photon-addition operation on $|\mu\rangle$ generates a state $|\mu^{(k)}\rangle$ orthogonal to the span of the set $\{|n\rangle : n \leq h\}$. If both $\xi = 0$ and $h = 0$, then $|\xi^{(h)}\rangle$ corresponds to the ground state, and therefore the QSD reduces to the discrimination between a PACS and the ground state. The orthogonality condition (8b) represents the situation in which there are canceling cross-terms in the scalar product of the two states. It can also be observed that the exponential factor in (7) makes the DEP vanish as $|\mu - \xi|$ increases. Therefore, in the absence of noise, the use of PACSs can provide an optimal solution to the QSD problem.

In the following, it is shown that the presence of thermal noise during state preparation increases the DEP. Since a noise component is unavoidable in quantum systems, it is essential to represent the noisy quantum states and characterize the QSD that accounts for thermal noise in state preparation.

III. Representation of Noisy Quantum States

This section provides the representation of noisy PACSs accounting for the presence of thermal noise during the preparation of the quantum states.

A. Noisy Coherent States

A noisy coherent state with amplitude $\mu \in \mathbb{C}$ is obtained by displacing the thermal state $\boldsymbol{\varXi}_{\text{th}}$ as

$$\boldsymbol{\varXi}_{\text{th}}(\mu) = \boldsymbol{D}_\mu \boldsymbol{\varXi}_{\text{th}} \boldsymbol{D}_\mu^\dagger. \quad (9)$$

The thermal state is given by [55]

$$\boldsymbol{\varXi}_{\text{th}} = \sum_{n=0}^{\infty} \frac{\bar{n}^n}{(1+\bar{n})^{n+1}} |n\rangle\langle n| \quad (10)$$

where $\bar{n}$ is the mean number of thermal photons given by Planck's law

$$\bar{n} = (\exp\{\hbar\omega/k_{\text{B}}T_0\} - 1)^{-1}$$

in which $\hbar$ is the reduced Planck constant, ω is the angular frequency of the field, k_{B} is the Boltzmann constant, and T_0 is the absolute temperature of the quantum system.

The Fock representation of a noisy coherent state $\boldsymbol{\varXi}_{\text{th}}(\mu)$ is given by [1]

$$\langle n|\boldsymbol{\varXi}_{\text{th}}(\mu)|m\rangle = (1-v)\, e^{-(1-v)|\mu|^2} \sqrt{\frac{n!}{m!}} \times v^n [(1-v)\mu^*]^{m-n} L_n^{m-n}\left(\frac{-(1-v)^2|\mu|^2}{v}\right) \quad (11)$$

where

$$v = \frac{\bar{n}}{1+\bar{n}}. \quad (12)$$

The Wigner W-function, the Glauber–Sudarshan P-function, and the Husimi–Kano Q-function associated with $\boldsymbol{\varXi}_{\text{th}}(\mu)$ are respectively given by [55]

$$W_{\text{th}}(\alpha) = \frac{1}{\pi(\bar{n}+\frac{1}{2})} \exp\left\{-\frac{|\alpha-\mu|^2}{\bar{n}+\frac{1}{2}}\right\} \quad (13)$$

$$P_{\text{th}}(\alpha) = \frac{1}{\pi\bar{n}} \exp\left\{-\frac{|\alpha-\mu|^2}{\bar{n}}\right\} \quad (14)$$

$$Q_{\text{th}}(\alpha) = \frac{1}{\pi(\bar{n}+1)} \exp\left\{-\frac{|\alpha-\mu|^2}{\bar{n}+1}\right\}. \quad (15)$$

For $\bar{n}$ approaching 0, $P_{\text{th}}(\alpha)$ tends to $\delta(\alpha_{\text{r}} - \mu_{\text{r}})\delta(\alpha_{\text{i}} - \mu_{\text{i}})$ and the noisy coherent state $\boldsymbol{\varXi}_{\text{th}}(\mu)$ reduces to the coherent state $|\mu\rangle\langle\mu|$.

B. Noisy Photon-Added Coherent States

Photon addition on a quantum state $\boldsymbol{\varXi}$ produces a new state given by [56]

$$\boldsymbol{\varXi}_+ = \frac{\boldsymbol{A}^\dagger \boldsymbol{\varXi} \boldsymbol{A}}{\text{tr}\{\boldsymbol{A}^\dagger \boldsymbol{\varXi} \boldsymbol{A}\}}.$$

If $\boldsymbol{\varXi}$ is a coherent state affected by thermal noise, the corresponding photon-added state $\boldsymbol{\varXi}_+$ is referred to as noisy PACS.[3] Therefore, a noisy PACS is defined as

$$\boldsymbol{\varXi}(\mu, k) = \frac{(\boldsymbol{A}^\dagger)^k \boldsymbol{\varXi}_{\text{th}}(\mu) \boldsymbol{A}^k}{N_k(\mu, \bar{n})} \quad (16)$$

where $k \in \mathbb{N}$ represents the number of addition operations, and $N_k(\mu, \bar{n}) = \text{tr}\{(\boldsymbol{A}^\dagger)^k \boldsymbol{\varXi}_{\text{th}}(\mu) \boldsymbol{A}^k\}$. From [38, eq. (7.16)], we obtain[4]

$$N_k(\mu, \bar{n}) = k!(\bar{n}+1)^k L_k\left(-\frac{|\mu|^2}{\bar{n}+1}\right). \quad (17)$$

Note that a noisy PACS is uniquely determined by the parameters k, μ, and $\bar{n}$; such dependencies will not be explicated unless strictly needed. The mean number of photons $n_{\text{p}}(\mu, \bar{n})$ in a noisy PACS is given by $\langle \boldsymbol{A}^\dagger \boldsymbol{A}\rangle$. Since

$$\langle \boldsymbol{A}^\dagger \boldsymbol{A}\rangle = \text{tr}\{\boldsymbol{\varXi}(\mu,k)\boldsymbol{A}^\dagger\boldsymbol{A}\} = \text{tr}\{\boldsymbol{\varXi}(\mu,k)\boldsymbol{A}\boldsymbol{A}^\dagger\} - 1$$

we found

$$n_{\text{p}}(\mu, \bar{n}) = \frac{N_{k+1}(\mu, \bar{n})}{N_k(\mu, \bar{n})} - 1. \quad (18)$$

[3]This definition of noisy PACS is in accordance with that of photon-added displaced thermal state (PADTS) in [50], a special case of a photon-added displaced squeezed thermal state [51], [52] with no squeezing. We then provide new representations, all in closed form, for PADTS.

[4]This result is in accordance with [50, eq. (7)] for $V = 2\bar{n} + 1$.

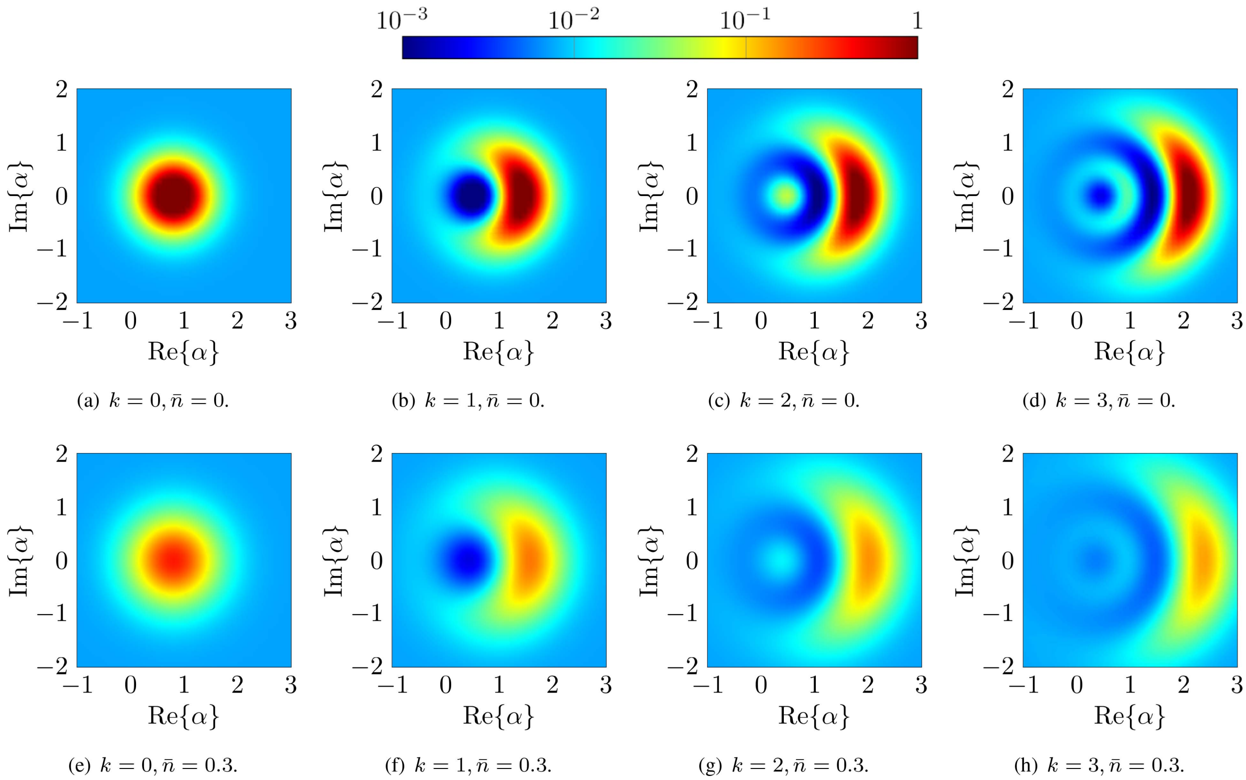

Fig. 2. Wigner W-function $W(\alpha)$ of a noisy PACS for different values of k and $\bar{n}$ with $\mu = 0.8$.

For a given noise level $\bar{n}$, the $n_{\mathrm{p}}(\mu, \bar{n})$ has a minimum at $\mu = 0$. From (18) and (17) such a minimum is given by

$$n_{\mathrm{p}}(0, \bar{n}) = (k+1)(\bar{n}+1) - 1. \tag{19}$$

In the following, the Fock representation, the Wigner W-function, the Glauber–Sudarshan P-function, and the Husimi–Kano Q-function are given for noisy PACS.

Theorem 1 (Fock representation): The Fock representation of a noisy PACS $\boldsymbol{\Xi}(\mu, k)$ is found to be

$$\langle n|\boldsymbol{\Xi}(\mu, k)|m\rangle = \begin{cases} c_{n,m}^{(k)} & \text{for both } n, m \geq k \\ 0 & \text{otherwise} \end{cases} \tag{20}$$

where $k \in \mathbb{N}$, and

$$c_{n,m}^{(k)} = \frac{(1-v)^{k+1} e^{-(1-v)|\mu|^2}}{v^k} \sqrt{\frac{n!}{m!}} \binom{m}{k} \times v^n [(1-v)\mu^*]^{m-n} \frac{L_{n-k}^{m-n}\left(\frac{-(1-v)^2|\mu|^2}{v}\right)}{L_k\left(-|\mu|^2(1-v)\right)}. \tag{21}$$

Proof: See Appendix B. □

The probability distribution for the number of photons n in a PACS $\boldsymbol{\Xi}(\mu, k)$ is obtained using Theorem 1 as

$$\mathbb{P}\{\mathsf{n} = n\} = \langle n|\boldsymbol{\Xi}(\mu, k)|n\rangle = \begin{cases} p_n^{(k)} & \text{for } n \geq k \\ 0 & \text{otherwise} \end{cases} \tag{22}$$

where $p_n^{(k)} = c_{n,n}^{(k)}$ is obtained from (21) with $m = n$. The following Theorems 2–4 provide a noisy PACS representation in terms of Wigner W-function, Glauber–Sudarshan P-function, and Husimi–Kano Q-function, respectively.

Theorem 2 (W-function): The Wigner W-function of a noisy PACS $\boldsymbol{\Xi}(\mu, k)$ is found to be

$$W(\alpha) = \frac{(-1)^k}{(2\bar{n}+1)^k} \frac{L_k\left(\frac{|2\alpha(\bar{n}+1)-\mu|^2}{(2\bar{n}+1)(\bar{n}+1)}\right)}{L_k\left(-\frac{|\mu|^2}{\bar{n}+1}\right)} W_{\mathrm{th}}(\alpha) \tag{23}$$

where $k \in \mathbb{N}$ and $W_{\mathrm{th}}(\alpha)$ is the Wigner W-function of a noisy coherent state given by (13).

Proof: See Appendix C. □

Fig. 2 shows $W(\alpha)$ for different values of k and $\bar{n}$. Notice that the Wigner function gets stretched and loses its negativity as $\bar{n}$ increases. Recalling that the negativity of the Wigner function is an indicator of non-classicality of the state [57], this behavior shows that the quantum state decoheres as the thermal noise increases.

Theorem 3 (P-function): The Glauber–Sudarshan P-function of a noisy PACS $\boldsymbol{\Xi}(\mu, k)$ is found to be

$$P(\alpha) = \frac{(-1)^k}{\bar{n}^k} \frac{L_k\left(\frac{|\alpha(\bar{n}+1)-\mu|^2}{\bar{n}(\bar{n}+1)}\right)}{L_k\left(-\frac{|\mu|^2}{\bar{n}+1}\right)} P_{\mathrm{th}}(\alpha) \tag{24}$$

where $k \in \mathbb{N}$ and $P_{\mathrm{th}}(\alpha)$ is the Glauber–Sudarshan P-function of a noisy coherent state given by (14).

Proof: See Appendix D. □

Theorem 4 (Q-function): The Husimi–Kano Q-function of a noisy PACS $\boldsymbol{\Xi}(\mu, k)$ is found to be

$$Q(\alpha) = \frac{|\alpha|^{2k}}{k!(\bar{n}+1)^k L_k\left(-\frac{|\mu|^2}{\bar{n}+1}\right)} Q_{\mathrm{th}}(\alpha). \tag{25}$$

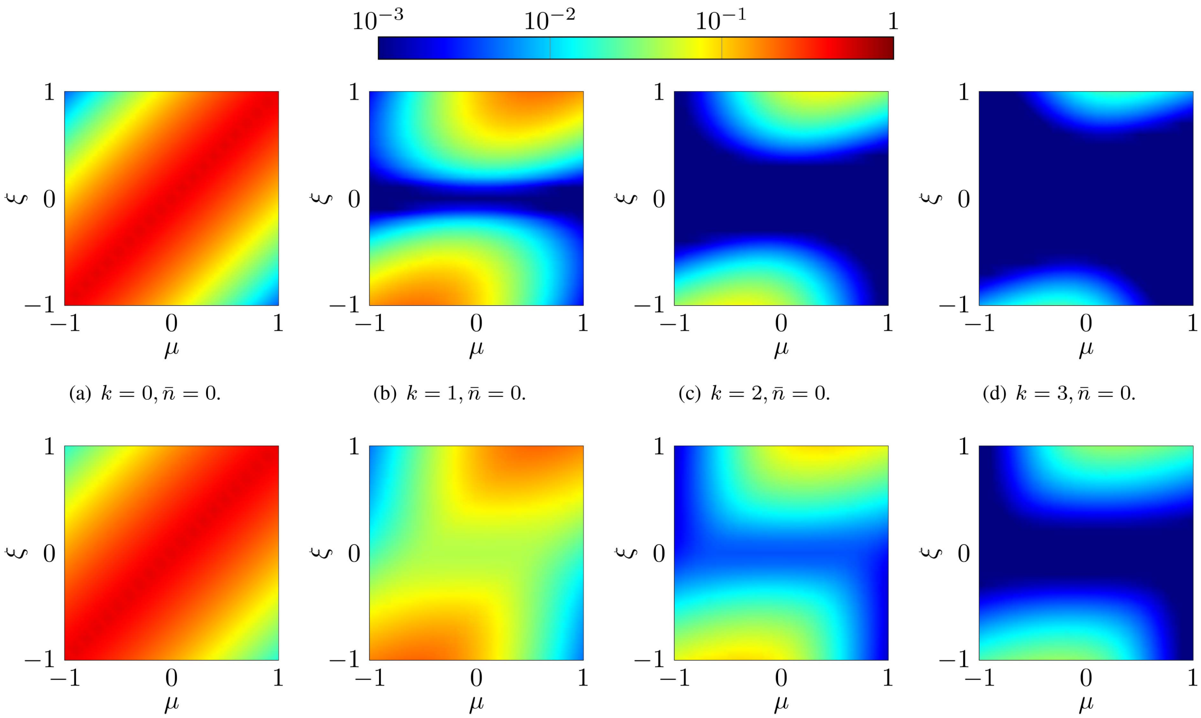

(a) $k=0, \bar{n}=0$. (b) $k=1, \bar{n}=0$. (c) $k=2, \bar{n}=0$. (d) $k=3, \bar{n}=0$.

(e) $k=0, \bar{n}=0.1$. (f) $k=1, \bar{n}=0.1$. (g) $k=2, \bar{n}=0.1$. (h) $k=3, \bar{n}=0.1$.

Fig. 3. MDEP for discrimination between a noisy PACS and a noisy coherent state as a function of μ and ξ, with $p_0 = p_1 = 1/2$.

where $k \in \mathbb{N}$ and $Q_{\text{th}}(\alpha)$ is the Husimi–Kano Q-function of a noisy coherent state given by (15).

Proof: See Appendix E. □

It is worth noting that the developed representation of a noisy PACS has relevant special cases. First, in case of no photon addition (i.e., $k = 0$) the representation of a noisy PACS reduces to that of a noisy coherent state, as described in Section III-A. Moreover, in the absence of noise (i.e., $\bar{n} = 0$), the representation of a noisy PACS reduces to that of a noiseless PACS presented in [45]. Furthermore, in the absence of displacement (i.e., $\mu = 0$), the representation of a noisy PACS reduces to that of a photon-added thermal state (PATS) presented in [58]. Finally, in the absence of both noise and displacement (i.e., $\bar{n} = \mu = 0$), the representation of a noisy PACS reduces to that of a Fock state shown in [55].

IV. Discrimination of Noisy Photon-Added Coherent States

This section characterizes the binary QSD with noisy PACSs using the representations given in Section III. In particular, the quantum states associated with the binary hypotheses in (1) are

$$\boldsymbol{\Xi}_0 = \boldsymbol{\Xi}(\xi, h) \tag{26a}$$

$$\boldsymbol{\Xi}_1 = \boldsymbol{\Xi}(\mu, k). \tag{26b}$$

Recall that, according to the Helstrom bound (3), the MDEP for a binary QSD depends on $\|\boldsymbol{\Delta}\|_1$ with $\boldsymbol{\Delta} = p_1\boldsymbol{\Xi}_1 - p_0\boldsymbol{\Xi}_0$. The following lemma shows that the MDEP for a binary QSD with quantum states as in (26) does not depend on the individual phases of ξ and μ, but only on the phase difference.

Lemma 2: Consider the PACSs $\boldsymbol{\Xi}_0 = \boldsymbol{\Xi}(\xi, h)$, $\boldsymbol{\Xi}_1 = \boldsymbol{\Xi}(\mu, k)$, $\boldsymbol{\Xi}_0^{(\theta)} = \boldsymbol{\Xi}(\xi e^{\imath\theta}, h)$, and $\boldsymbol{\Xi}_1^{(\phi)} = \boldsymbol{\Xi}(\mu e^{\imath\phi}, k)$ with $\theta, \phi \in \mathbb{R}$, defined as in (16). Then,

$$\|p_1\boldsymbol{\Xi}_1^{(\phi)} - p_0\boldsymbol{\Xi}_0^{(\theta)}\|_1 = \|p_1\boldsymbol{\Xi}_1 - p_0\boldsymbol{\Xi}_0^{(\theta-\phi)}\|_1. \tag{27}$$

Proof: See Appendix F. □

This result simplifies the QSD characterization, especially when one of the states is the thermal state for which the phase is irrelevant, as shown in the following corollary.

Corollary 1: Consider the PACSs of Lemma 2 with $\xi = h = 0$, for which $\boldsymbol{\Xi}_0 = \boldsymbol{\Xi}_{\text{th}}$. Then,

$$\|p_1\boldsymbol{\Xi}_1^{(\phi)} - p_0\boldsymbol{\Xi}_0^{(\theta)}\|_1 = \|p_1\boldsymbol{\Xi}_1 - p_0\boldsymbol{\Xi}_{\text{th}}\|_1. \tag{28}$$

Proof: From $\boldsymbol{\Xi}_0^{(\theta-\phi)} = \boldsymbol{R}_{\theta-\phi}\boldsymbol{\Xi}_{\text{th}}\boldsymbol{R}_{\theta-\phi}^{\dagger}$ and rotational invariance of $\boldsymbol{\Xi}_{\text{th}}$, the (27) reduces to (28). □

The operator $\boldsymbol{\Delta}$ has an infinite number of eigenvalues that have no closed-form expression. This is a long standing problem [1] and a tractable approximation of $\boldsymbol{\Delta}$ is needed to compute the MDEP. A simple way to approximate $\boldsymbol{\Delta}$ is to use an operator $\tilde{\boldsymbol{\Delta}}_N$, of finite dimension N, in the Fock representation. In particular, $\boldsymbol{\Delta} \simeq \tilde{\boldsymbol{\Delta}}_N$ where

$$\tilde{\boldsymbol{\Delta}}_N = \sum_{n=0}^{N-1}\sum_{m=0}^{N-1} \langle n|\boldsymbol{\Delta}|m\rangle |n\rangle\langle m|$$

with entries $\langle n|\boldsymbol{\Delta}|m\rangle$ obtained using (20). The accuracy of MDEP approximation using $\tilde{\boldsymbol{\Delta}}_N$ depends on N.[5]

[5] $N = 30$ will be used in the remainder of the paper.

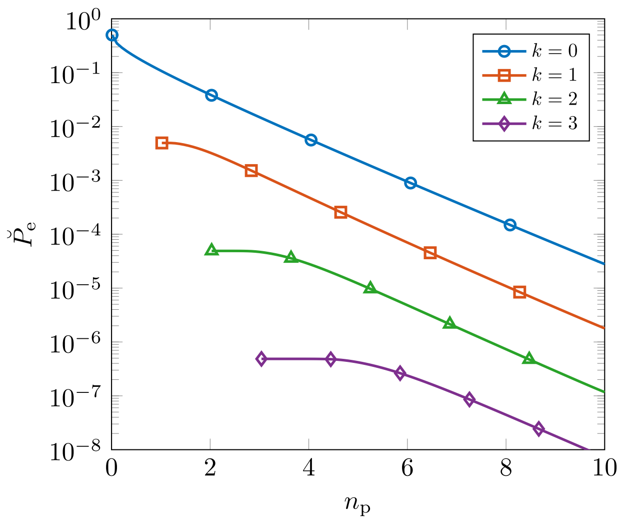

(a) MDEP with optimal discriminator (quantum).

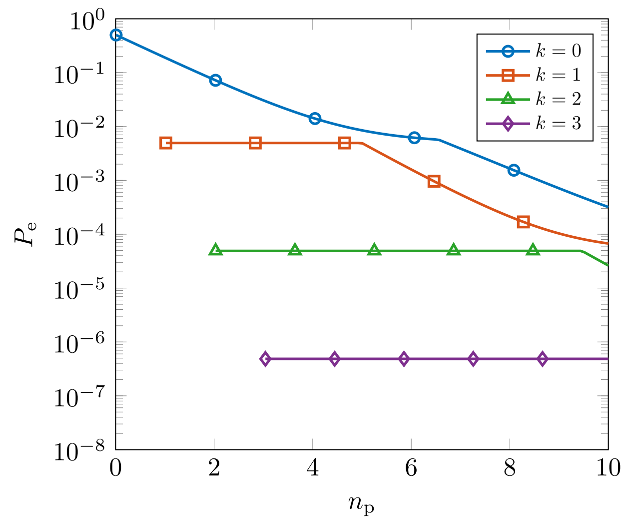

(b) DEP with counting discriminator (classical).

Fig. 4. Performance of the QSD between a noisy PACS and the thermal state as a function of n_p, with $\bar{n} = 10^{-2}$, and $p_0 = p_1 = 1/2$.

A. Case Studies

To quantify the noise effects on QSD, two case studies will be considered.

1) $\varXi_0$ noisy coherent state, $\varXi_1$ noisy PACS: The quantum states associated with the binary hypotheses in (1) are

$$\varXi_0 = \varXi(\xi, 0)$$
$$\varXi_1 = \varXi(\mu, k).$$

Recall from (3) and Lemma 2 that, since $h = 0$, the MDEP only depends on $\bar{n}$, k, $|\xi|$, $|\mu|$, and $\arg(\xi) - \arg(\mu)$.

Fig. 3 shows the MDEP as a function of μ and ξ, for different values of k and $\bar{n}$.[6] Note that, for $\bar{n} \neq 0$, the MDEP is always greater than zero and, differently from (8a) in the noiseless case, $\xi = 0$ is no longer an optimal solution.

2) $\varXi_0$ thermal state, $\varXi_1$ noisy PACS: The quantum states associated with the binary hypotheses in (1) are

$$\varXi_0 = \varXi(0, 0)$$
$$\varXi_1 = \varXi(\mu, k).$$

Recall from (3) and Corollary 1 that the MDEP only depends on $\bar{n}$, k, and $|\mu|$.

Fig. 4(a) shows the MDEP as a function of the mean number n_p of photons in $\varXi_1$, for different values of k. Note that the use of a PACS improves the QSD performance compared to the use of a coherent state ($k = 0$). Moreover, the performance improves with the number of photon addition operations, which is inversely proportional to the state generation efficiency. Therefore, there is a trade-off between the MDEP and the state generation rate. Furthermore, the minimum value of n_p is given by (19).

Consider also the case of counting discriminator, which simply counts the number of photons in the quantum state and compares it with a threshold that depends on the state $\varXi_1$. The counting discriminator is more feasible than the optimal discriminator and admits a purely classical description [59].

[6]While ξ and μ are complex in general, here they are plotted for real values.

Fig. 4(b) shows the DEP of a counting discriminator as a function of the mean number n_p of photons in $\varXi_1$, for different values of k. In comparison to Fig. 4(a), it can be observed that the DEP with a counting discriminator is higher than that of the optimal quantum discriminator (i.e., the MDEP), as expected. Note that the use of a PACS improves the QSD performance compared to the use of a coherent state ($k = 0$), even for the counting discriminator. Note also that the DEP of a counting discriminator approaches the MDEP for low values of n_p. This can be attributed to the fact that, when n_p is low the off-diagonal terms in the Fock representation, hence the quantum advantage, of a PACS vanish.

Fig. 5 shows the quantum gain ζ, the ratio between the DEP with a counting discriminator and the MDEP with the optimal discriminator, as a function of n_p, for different values of k. Note that the use of the optimal quantum discriminator always allows for improvement of the performance with respect to a classical discriminator.

Fig. 6 shows the MDEP as a function of the mean number $\bar{n}$ of thermal photons, for different values of k and for fixed $n_\mathrm{p} = 8$. Note that the use of a PACS improves the QSD performance compared to the use of a coherent state ($k = 0$), especially for small $\bar{n}$. Therefore, PACSs are particularly valuable in situations when thermal noise is low.

B. Application to Quantum Communications

A direct application of QSD is the transmission of classical information. A classical source generates a symbol a, from a finite alphabet $\mathcal{A} = \{a_0, a_1, \ldots, a_{M-1}\}$, with prior probabilities $\mathbb{P}\{\mathsf{a} = a_i\} = p_i$ for $i = 0, 1, \ldots, M-1$. When the source generates the symbol a_i, the transmitter prepares a quantum state $\varXi_i$, and sends it to the receiver through a physical channel. The set of all the quantum states $\mathcal{A}_\mathrm{q} = \{\varXi_0, \varXi_1, \ldots, \varXi_{M-1}\}$ is referred to as quantum constellation [5]. The prepared state traverses a quantum channel, mathematically described by a completely positive trace preserving map $\mathcal{C}$, which transforms the transmitted state $\varXi_i$ into $\boldsymbol{\Upsilon}_i = \mathcal{C}\{\varXi_i\}$. At the receiver side, the quantum state is

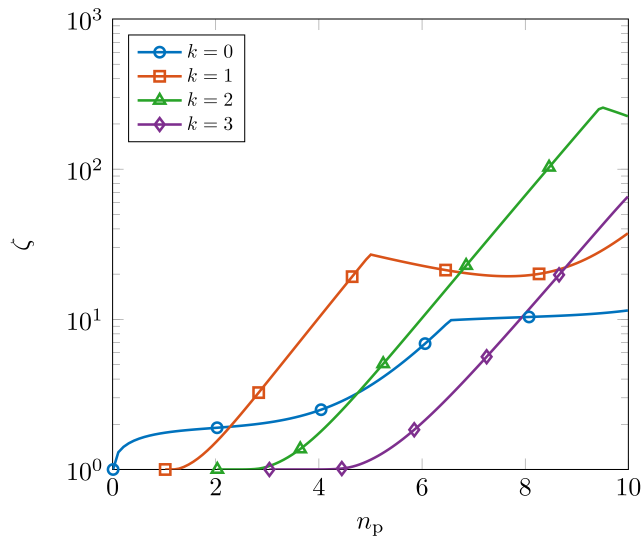

Fig. 5. Quantum gain ζ as a function of n_{p}, with $\bar{n} = 10^{-2}$, and $p_0 = p_1 = 1/2$.

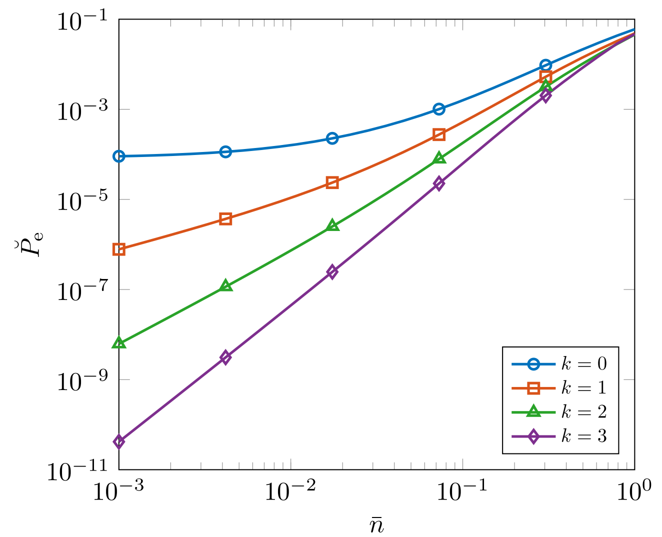

Fig. 6. MDEP for the discrimination between a noisy PACS and the thermal state as a function of $\bar{n}$, with $n_{\mathrm{p}} = 8$, and $p_0 = p_1 = 1/2$.

converted back to classical information by means of a quantum measurement and a decision is made to infer the transmitted symbol.

Consider a quantum on-off keying (OOK) system, which employs a binary alphabet ($M = 2$) and discriminates between $\boldsymbol{\Xi}_0 = \boldsymbol{\Xi}_{\mathrm{th}}$ and an arbitrary state $\boldsymbol{\Xi}_1$. In practice, the quantum source (e.g., a laser) prepares the state $\boldsymbol{\Xi}_1$ when the symbol a_1 is emitted, and the quantum source is turned off when the symbol a_0 is emitted. The MDEP of an OOK system employing a PACS corresponds to the MDEP studied in Section IV-A2.

V. The Effect of Decoherence

This section quantifies the effects of a quantum channel (i.e., phase diffusion and photon loss) on the QSD performance. The quantum states associated with the binary hypotheses in (1) are

$$\boldsymbol{\Upsilon}_0 = \mathcal{C}\{\boldsymbol{\Xi}(0,0)\}$$
$$\boldsymbol{\Upsilon}_1 = \mathcal{C}\{\boldsymbol{\Xi}(\mu,k)\}$$

where $\boldsymbol{\Upsilon} = \mathcal{C}\{\boldsymbol{\Xi}\}$ is the state at the output of the quantum channel described by $\mathcal{C}\{\cdot\}$ with input $\boldsymbol{\Xi}$.

A. Phase Diffusion

The phase diffusion model [55] is a purely quantum mechanical model that has no classical counterparts and can be used to model different phenomena (e.g., the random scattering of photons in a waveguide). In the presence of phase diffusion, the quantum state $\boldsymbol{\Xi}$ becomes $\boldsymbol{\Upsilon}$ such that

$$\langle n|\boldsymbol{\Upsilon}|m\rangle = e^{-(n-m)^2\sigma^2}\langle n|\boldsymbol{\Xi}|m\rangle$$

where σ is the phase diffusion parameter. Therefore, the effect of phase diffusion is the exponential damping of the off-diagonal elements in the Fock representation. Note that this model can be used to describe the reception of a state with unknown phase. For example, when the phase of a state is unknown, a uniform random model is used [22] and the evolution $\boldsymbol{\Upsilon}$ of state $\boldsymbol{\Xi}$ results in

$$\boldsymbol{\Upsilon} = \int_0^{2\pi} \frac{1}{2\pi} \boldsymbol{R}_\phi \boldsymbol{\Xi} \boldsymbol{R}_\phi^\dagger \, d\phi.$$

In such a case, $\langle n|\boldsymbol{\Upsilon}|m\rangle = \delta_{n,m}\langle n|\boldsymbol{\Xi}|m\rangle$, which resembles to the phase diffusion model with large σ (high-phase diffusion), for which $\boldsymbol{\Upsilon}$ reduces to a purely classical state.

We now quantify the effects of phase diffusion on the MDEP as described in Section IV. Fig. 7 shows the MDEP as a function of σ^2 for different values of k. Note that the use of a PACS improves the QSD performance compared to the use of a coherent state ($k = 0$). It can be observed that, for small σ, MDEP with phase diffusion approaches to that without phase diffusion. It can also be observed that, for large σ, the MDEP with the optimal discriminator approaches the DEP with a counting discriminator as the off-diagonal terms vanish. Therefore, in the presence of a strong phase diffusion, the counting discriminator is asymptotically optimal. This can be attributed to the fact that the off-diagonal terms in the Fock representation vanish as the diffusion parameter increases.

B. Photon Loss

The photon loss model [60] describes the energy loss of a photon due to propagation from source to destination, and it can be used to model different phenomena (e.g., the free-space propagation). In the presence of photon loss, the quantum state $\boldsymbol{\Xi}$ becomes $\boldsymbol{\Upsilon}$ such that

$$\langle n|\boldsymbol{\Upsilon}|m\rangle = \frac{1}{\eta^2\sqrt{n!m!}} \iint P_{\boldsymbol{\Xi}}\left(\frac{\alpha}{\eta}\right) e^{-|\alpha|^2} (\alpha^*)^n \alpha^m \, d\alpha_{\mathrm{r}} \, d\alpha_{\mathrm{i}}$$

where $\eta \in [0,1]$ is the transmissivity parameter. Therefore, the effect of photon loss is a joint attenuation and scaling of the P-function.

We now quantify the effects of photon loss on the MDEP as described in Section IV. Fig. 8 shows the MDEP as a function of η for different values of k. Note that the use of a PACS improves the QSD performance compared to the use of

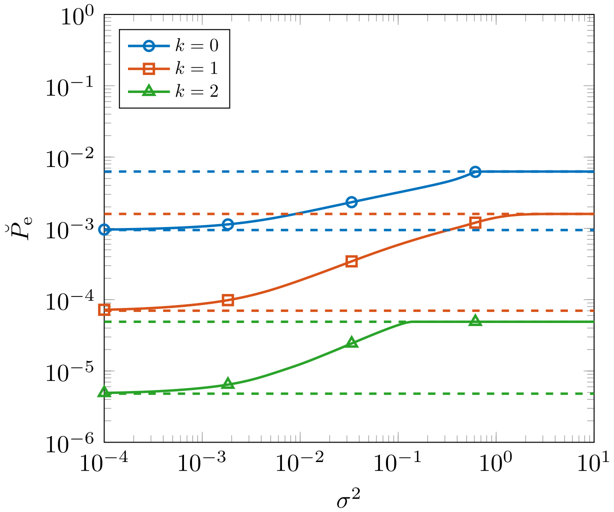

Fig. 7. MDEP for the discrimination between a noisy PACS and the thermal state affected by phase diffusion as a function of σ^2, with $n_{\rm p}=6$, $\bar{n}=10^{-2}$, and $p_0=p_1=1/2$. The two dashed lines for each k represent the MDEP without phase noise (bottom) and the DEP of a counting discriminator (top).

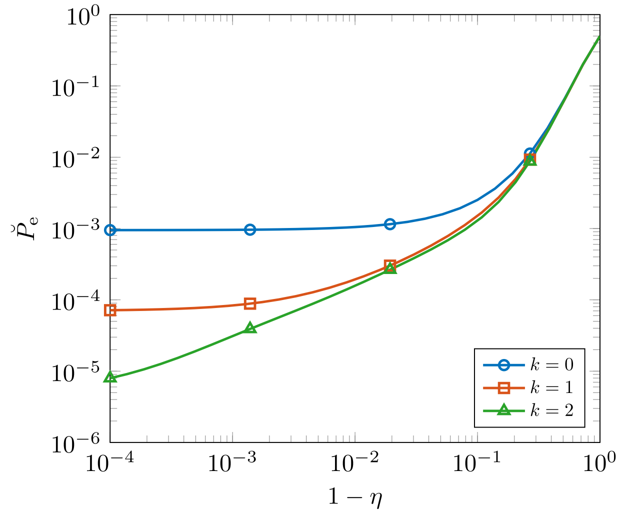

Fig. 8. MDEP for the discrimination between a noisy PACS and the thermal state affected by photon loss as a function of η, with $n_{\rm p}=6$, $\bar{n}=10^{-2}$, and $p_0=p_1=1/2$.

a coherent state ($k=0$), especially for high η. Note also that, in the high-loss regime (i.e., when $\eta\approx 0$), MDEP with a PACS approaches to that with a coherent state for all k. Therefore, PACSs are particularly valuable in situations when the loss is low. This can be attributed to the fact that the quantum state loses its non-classical properties more rapidly as η decreases.

VI. Conclusion

This paper addresses the problem of discriminating between two noisy PACSs. First, the representation of PACSs affected by thermal noise during state preparation is given in terms of Fock basis, Wigner W-function, Glauber–Sudarshan P-function, and Husimi–Kano Q-function. Then, it is shown that the use of PACSs instead of coherent states with the same energy can significantly improve the QSD performance. It is also shown how this advantage depends on the decoherence and the losses in the system. The findings of this paper open the way for the use of non-coherent states, in particular PACSs, for QSD applications.

Appendix A
Proof of Lemma 1

From (6) and the normalization in [45],

$$\langle\xi^{(h)}|\mu^{(k)}\rangle=\frac{\langle\xi|\boldsymbol{A}^h(\boldsymbol{A}^\dagger)^k|\mu\rangle}{\sqrt{h!k!L_k(-|\mu|^2)L_h(-|\xi|^2)}}. \tag{29}$$

The enumerator of (29) can be written as

$$\begin{aligned}\langle\xi|\boldsymbol{A}^h(\boldsymbol{A}^\dagger)^k|\mu\rangle&=\langle\xi|\mu\rangle\sum_{n=0}^{h}n!\binom{k}{n}\binom{h}{n}\mu^{h-n}(\xi^*)^{k-n}\\&=\langle\xi|\mu\rangle h!(\xi^*)^{k-h}\sum_{n=0}^{h}\binom{k}{h-n}\frac{(\mu\xi^*)^n}{n!}\\&=\langle\xi|\mu\rangle h!(\xi^*)^{k-h}L_h^{k-h}(-\mu\xi^*) \qquad (30)\end{aligned}$$

where the first equality is obtained by using [37, eq. (5.12)] to express $\boldsymbol{A}^h(\boldsymbol{A}^\dagger)^k$ in the normal order and noticing that $\boldsymbol{A}|\mu\rangle=\mu|\mu\rangle$ when $|\mu\rangle$ is a coherent state; the second equality follows from simple algebra; and the third equality follows from the definition of generalized Laguerre polynomials. From (30), and [36, eq. (3.32)], the (29) results in (7).

Appendix B
Proof of Theorem 1

The coherent-state representation of a noisy PACS $\boldsymbol{\Xi}(\mu,k)$, defined as [36, eq. (6.1)], can be written as

$$R(\alpha^*,\beta)=e^{\frac{1}{2}(|\alpha|^2+|\beta|^2)}\langle\alpha|\boldsymbol{\Xi}(\mu,k)|\beta\rangle.$$

From (16),

$$\begin{aligned}R(\alpha^*,\beta)&=\frac{e^{\frac{1}{2}(|\alpha|^2+|\beta|^2)}}{N_k}\langle\alpha|(\boldsymbol{A}^\dagger)^k\boldsymbol{D}_\mu\boldsymbol{\Xi}_{\rm th}\boldsymbol{D}_\mu^\dagger\boldsymbol{A}^k|\beta\rangle\\&=\frac{(\alpha^*\beta)^k}{N_k}\,e^{\frac{1}{2}(|\alpha|^2+|\beta|^2)}\langle\alpha|\boldsymbol{D}_\mu\boldsymbol{\Xi}_{\rm th}\boldsymbol{D}_\mu^\dagger|\beta\rangle \qquad (31)\end{aligned}$$

where the first equality is from (16) and (9), and the second equality follows from the fact that a coherent state is an eigenvector of $\boldsymbol{A}$. From the coherent-state representation of a displaced thermal state [1, eq. (4.15)] together with (17) and (12), the (31) becomes

$$\begin{aligned}R(\alpha^*,\beta)&=\frac{(\alpha^*\beta)^k(1-v)^{k+1}}{k!L_k(-|\mu|^2(1-v))}\exp\{-(1-v)|\mu|^2\}\\&\quad\times\exp\{v\alpha^*\beta+(1-v)(\alpha^*\mu+\beta\mu^*)\}. \qquad (32)\end{aligned}$$

From the Mollow–Glauber double generating function for the associated Laguerre polynomials [61, eqs. (A1) and (A6)] and by applying some simple algebra, the (32) results in

$$\begin{aligned}R(\alpha^*,\beta)=&\sum_{n=k}^{\infty}\sum_{m=k}^{\infty}\frac{(\alpha^*)^n\beta^m}{\sqrt{n!m!}}\frac{(1-v)^{k+1}}{L_k(-|\mu|^2(1-v))v^k}\\&\times\exp\{-(1-v)|\mu|^2\}\sqrt{\frac{n!}{m!}}\binom{m}{k}v^n\\&\times[(1-v)\mu^*]^{m-n}L_{n-k}^{m-n}\left(-\frac{(1-v)^2|\mu|^2}{v}\right).\end{aligned} \tag{33}$$

$$W(\alpha) = \frac{2(1-v)^{k+1} e^{2|\alpha|^2-(1-v)|\mu|^2}}{\pi^2 k!\, L_k(-|\mu|^2(1-v))} \iint (-\beta^*\beta)^k\, e^{-(1+v)|\beta|^2+\beta^*(2\alpha-(1-v)\mu)-\beta(2\alpha-(1-v)\mu)^*}\, d\beta_{\mathrm{r}}\, d\beta_{\mathrm{i}} \tag{36}$$

$$P(\alpha) = \frac{(1-v)^{k+1} e^{|\alpha|^2-(1-v)|\mu|^2}}{\pi^2 k!\, L_k(-|\mu|^2(1-v))} \iint (-\beta^*\beta)^k\, e^{-v|\beta|^2+\beta^*(\alpha-(1-v)\mu)-\beta(\alpha-(1-v)\mu)^*}\, d\beta_{\mathrm{r}}\, d\beta_{\mathrm{i}} \tag{42}$$

From the relationship between coherent-state representation (33) and Fock representation [36, eq. (6.2)], the (20) is obtained.

Appendix C
Proof of Theorem 2

The Wigner W-function of a noisy PACS $\boldsymbol{\Xi}(\mu,k)$, defined according to [45, eq. (3.5)], can be written as

$$W(\alpha) = \frac{2\, e^{2|\alpha|^2}}{\pi^2} \iint \langle -\beta|\boldsymbol{\Xi}(\mu,k)|\beta\rangle\, e^{2(\beta^*\alpha-\beta\alpha^*)}\, d\beta_{\mathrm{r}}\, d\beta_{\mathrm{i}}. \tag{34}$$

From (31),

$$\langle -\beta|\boldsymbol{\Xi}(\mu,k)|\beta\rangle = R(-\beta^*,\beta)\, e^{-|\beta|^2} \tag{35}$$

and by using it together with (32) in (34), the (36) at the top of the page is obtained. Then, by applying a double change of variable

$$\gamma = \beta\sqrt{1+v} \tag{37a}$$

$$\xi = \frac{2\alpha-(1-v)\mu}{\sqrt{1+v}} \tag{37b}$$

we obtain

$$W(\alpha) = \frac{2(1-v)^{k+1} e^{2|\alpha|^2-(1-v)|\mu|^2}}{\pi k!\, L_k(-|\mu|^2(1-v))(1+v)^{k+1}}\, I^{(k)}(\xi) \tag{38}$$

where

$$I^{(k)}(\xi) = \frac{1}{\pi} \iint (-\gamma^*\gamma)^k\, e^{-|\gamma|^2+\gamma^*\xi-\gamma\xi^*}\, d\gamma_{\mathrm{r}}\, d\gamma_{\mathrm{i}}.$$

Using [62, eq. (A.28)] and the Wirtinger derivatives[7] [63],

$$I^{(k)}(\xi) = \frac{\partial^{2k}}{\partial\xi^{*k}\,\partial\xi^k}\, e^{-|\xi|^2}$$

and, from the definition of Laguerre polynomials,

$$I^{(k)}(\xi) = (-1)^k k!\, e^{-|\xi|^2} L_k(|\xi|^2). \tag{39}$$

From (39), the (38) can be rewritten as

$$W(\alpha) = \frac{(v-1)^k L_k(|\xi|^2)}{(1+v)^k L_k(-|\mu|^2(1-v))} \times \frac{2(1-v)\, e^{-|\xi|^2} e^{2|\alpha|^2-(1-v)|\mu|^2}}{\pi(1+v)}. \tag{40}$$

From (37b) together with (12) and (13), the (40) results in (23).

[7]Recall that the Wirtinger derivatives are defined as $\frac{\partial}{\partial\xi} = \frac{1}{2}(\frac{\partial}{\partial\xi_{\mathrm{r}}} - \imath\frac{\partial}{\partial\xi_{\mathrm{i}}})$ and $\frac{\partial}{\partial\xi^*} = \frac{1}{2}(\frac{\partial}{\partial\xi_{\mathrm{r}}} + \imath\frac{\partial}{\partial\xi_{\mathrm{i}}})$, from which $\frac{\partial}{\partial\xi}(\xi^*)^k = 0$ and $\frac{\partial}{\partial\xi^*}(\xi)^k = 0$ for $k \in \mathbb{N}$.

Appendix D
Proof of Theorem 3

The Glauber–Sudarshan P-function of a noisy PACS $\boldsymbol{\Xi}(\mu,k)$, defined according to [64, eq. (6)], can be written as

$$P(\alpha) = \frac{e^{|\alpha|^2}}{\pi^2} \iint \langle -\beta|\boldsymbol{\Xi}(\mu,k)|\beta\rangle\, e^{|\beta|^2} e^{\beta^*\alpha-\beta\alpha^*}\, d\beta_{\mathrm{r}}\, d\beta_{\mathrm{i}}. \tag{41}$$

Using (32) and (35) in (41), the (42) at the top of the page is obtained. Then, by applying a double change of variable

$$\gamma = \sqrt{v}\beta \tag{43a}$$

$$\xi = \frac{\alpha-(1-v)\mu}{\sqrt{v}} \tag{43b}$$

we obtain

$$P(\alpha) = \frac{(1-v)^{k+1} e^{|\alpha|^2-(1-v)|\mu|^2}}{\pi^2 k!\, L_k(-|\mu|^2(1-v))v^{k+1}}\, I^{(k)}(\xi). \tag{44}$$

From (39), (44) can be written as

$$P(\alpha) = \frac{(v-1)^k L_k(|\xi|^2)}{v^k L_k(-|\mu|^2(1-v))} \times \frac{(1-v)\, e^{-|\xi|^2} e^{|\alpha|^2-(1-v)|\mu|^2}}{\pi v}. \tag{45}$$

From (43b) together with (12) and (14), the (45) results in (24).

Appendix E
Proof of Theorem 4

The Husimi–Kano Q-function of a noisy PACS $\boldsymbol{\Xi}(\mu,k)$, defined according to [65, eq. (12.7)], can be written as

$$Q(\alpha) = \frac{1}{\pi}\langle\alpha|\boldsymbol{\Xi}(\mu,k)|\alpha\rangle. \tag{46}$$

From (31),

$$Q(\alpha) = \frac{e^{-|\alpha|^2}}{\pi} R(\alpha^*,\alpha). \tag{47}$$

From (32) together with (12) and (15), the (47) results in (25).

Appendix F
Proof of Lemma 2

From (16) and (9),

$$\boldsymbol{\Xi}_1^{(\phi)} = \frac{1}{N_k}(\boldsymbol{A}^\dagger)^k \boldsymbol{D}_\nu \boldsymbol{\Xi}_{\mathrm{th}} \boldsymbol{D}_\nu^\dagger \boldsymbol{A}^k$$

where $\nu = \mu e^{\imath\phi}$. By using the relationships between the operators $\boldsymbol{A}$, $\boldsymbol{A}^\dagger$, $\boldsymbol{D}_\mu$, and $\boldsymbol{R}_\phi$ [66], we obtain

$$\begin{aligned}\boldsymbol{\Xi}_1^{(\phi)} &= \frac{1}{N_k}(\boldsymbol{A}^\dagger)^k \boldsymbol{R}_\phi \boldsymbol{D}_\mu \boldsymbol{\Xi}_{\text{th}} \boldsymbol{D}_\mu^\dagger \boldsymbol{R}_\phi^\dagger \boldsymbol{A}^k \\ &= \frac{1}{N_k}\boldsymbol{R}_\phi (\boldsymbol{A}^\dagger)^k \boldsymbol{D}_\mu \boldsymbol{\Xi}_{\text{th}} \boldsymbol{D}_\mu^\dagger \boldsymbol{A}^k \boldsymbol{R}_\phi^\dagger \\ &= \boldsymbol{R}_\phi \boldsymbol{\Xi}_1 \boldsymbol{R}_\phi^\dagger \end{aligned} \tag{48}$$

where the first equality follows from $\boldsymbol{R}_\phi \boldsymbol{D}_\mu \boldsymbol{R}_\phi^\dagger = \boldsymbol{D}_\nu$ and the rotational invariance of $\boldsymbol{\Xi}_{\text{th}}$ for which $\boldsymbol{R}_\phi^\dagger \boldsymbol{\Xi}_{\text{th}} \boldsymbol{R}_\phi = \boldsymbol{\Xi}_{\text{th}}$; the second equality follows from $\boldsymbol{R}_\phi^\dagger \boldsymbol{A} \boldsymbol{R}_\phi = \boldsymbol{A} e^{-\imath\phi}$; and the third equality follows from the definition of $\boldsymbol{\Xi}_1$. Therefore, by using (48) for both $\boldsymbol{\Xi}_1^{(\phi)}$ and $\boldsymbol{\Xi}_0^{(\theta)}$ in the left-hand side of (27),

$$\begin{aligned}\|p_1 \boldsymbol{\Xi}_1^{(\phi)} - p_0 \boldsymbol{\Xi}_0^{(\theta)}\|_1 &= \|p_1 \boldsymbol{R}_\phi \boldsymbol{\Xi}_1 \boldsymbol{R}_\phi^\dagger - p_0 \boldsymbol{R}_\theta \boldsymbol{\Xi}_0 \boldsymbol{R}_\theta^\dagger\|_1 \\ &= \|p_1 \boldsymbol{\Xi}_1 - p_0 \boldsymbol{R}_{\theta-\phi} \boldsymbol{\Xi}_0 \boldsymbol{R}_{\theta-\phi}^\dagger\|_1 \end{aligned} \tag{49}$$

where the last equality follows from the isometric invariance of the trace norm [53], and $\boldsymbol{R}_\phi^\dagger = \boldsymbol{R}_{-\phi}$. From the definition of $\boldsymbol{\Xi}_0^{(\theta-\phi)}$, the (49) results in (27).

Acknowledgment

The authors wish to thank R. Cohen for the careful reading of the manuscript.

References

[1] C. W. Helstrom, *Quantum Detection and Estimation Theory*. New York, NY, USA: Academic Press, 1976.
[2] A. S. Holevo, "Statistical decision theory for quantum systems," *J. Multivariate Anal.*, vol. 3, no. 4, pp. 337–394, 1973.
[3] H. P. Yuen, R. S. Kennedy, and M. Lax, "Optimum testing of multiple hypotheses in quantum detection theory," *IEEE Trans. Inf. Theory*, vol. 21, no. 2, pp. 125–134, Mar. 1975.
[4] C. W. Helstrom, J. W. S. Liu, and J. P. Gordon, "Quantum-mechanical communication theory," *Proc. IEEE*, vol. 58, no. 10, pp. 1578–1598, Oct. 1970.
[5] G. Cariolaro, *Quantum Communications*. Heidelberg, Germany: Springer, 2015.
[6] W. C. Lindsey, "Transmission of classical information over noisy quantum channels—A spectrum approach," *IEEE J. Sel. Areas Commun.*, vol. 38, no. 3, pp. 427–438, Mar. 2020.
[7] C. L. Degen, F. Reinhard, and P. Cappellaro, "Quantum sensing," *Rev. Mod. Phys.*, vol. 89, Jul. 2017, Art. no. 035002.
[8] V. Giovannetti, S. Lloyd, and L. Maccone, "Quantum-enhanced measurements: Beating the standard quantum limit," *Science*, vol. 306, no. 5700, pp. 1330–1336, 2004.
[9] M. Paris, "Quantum estimation for quantum technology," *Int. J. Quantum Inf.*, vol. 7, no. 1, pp. 125–137, 2009.
[10] S. Lloyd, "Enhanced sensitivity of photodetection via quantum illumination," *Science*, vol. 321, no. 5895, pp. 1463–1465, 2008.
[11] S.-H. Tan *et al.*, "Quantum illumination with Gaussian states," *Phys. Rev. Lett.*, vol. 101, Dec. 2008, Art. no. 253601.
[12] E. D. Lopaeva, I. Ruo Berchera, I. P. Degiovanni, S. Olivares, G. Brida, and M. Genovese, "Experimental realization of quantum illumination," *Phys. Rev. Lett.*, vol. 110, Apr. 2013, Art. no. 153603.
[13] N. Gisin, G. Ribordy, W. Tittel, and H. Zbinden, "Quantum cryptography," *Rev. Mod. Phys.*, vol. 74, pp. 145–195, Mar. 2002.
[14] V. Scarani, H. Bechmann-Pasquinucci, N. J. Cerf, M. Dušek, N. Lütkenhaus, and M. Peev, "The security of practical quantum key distribution," *Rev. Mod. Phys.*, vol. 81, pp. 1301–1350, Sep. 2009.
[15] S. Guerrini, M. Chiani, and A. Conti, "Secure key throughput of intermittent trusted-relay QKD protocols," in *Proc. IEEE Workshop Quantum Commun. Inf. Technol. (QCIT) Global Telecommun. Conf.*, Abu Dhabi, UAE, Dec. 2018, pp. 1–5.
[16] G. Chiribella, G. M. D'Ariano, and P. Perinotti, "Theoretical framework for quantum networks," *Phys. Rev. A*, vol. 80, Aug. 2009, Art. no. 022339.
[17] H. J. Kimble, "The quantum Internet," *Nature*, vol. 453, no. 7198, pp. 1023–1030, Jun. 2008.
[18] W. Dai, T. Peng, and M. Z. Win, "Quantum queuing delay," *IEEE J. Sel. Areas Commun.*, vol. 38, no. 3, pp. 605–618, Mar. 2020.
[19] M. A. Nielsen and I. L. Chuang, *Quantum Computation and Quantum Information*. Cambridge, U.K.: Cambridge University Press, 2010.
[20] R. Cleve, A. Ekert, C. Macchiavello, and M. Mosca, "Quantum algorithms revisited," *Proc. Roy. Soc. London A*, vol. 454, no. 1969, pp. 339–354, 1998.
[21] J. A. Bergou, U. Herzog, and M. Hillery, "Quantum filtering and discrimination between sets of Boolean functions," *Phys. Rev. Lett.*, vol. 90, Jun. 2003, Art. no. 257901.
[22] S. L. Braunstein and P. van Loock, "Quantum information with continuous variables," *Rev. Mod. Phys.*, vol. 77, pp. 513–577, Jun. 2005.
[23] C. Weedbrook *et al.*, "Gaussian quantum information," *Rev. Mod. Phys.*, vol. 84, pp. 621–669, May 2012.
[24] T. C. Ralph, A. Gilchrist, G. J. Milburn, W. J. Munro, and S. Glancy, "Quantum computation with optical coherent states," *Phys. Rev. A*, vol. 68, no. 4, 2003, Art. no. 042319.
[25] H. Yonezawa, T. Aoki, and A. Furusawa, "Demonstration of a quantum teleportation network for continuous variables," *Nature*, vol. 431, no. 7007, pp. 430–433, 2004.
[26] P. Jouguet, S. Kunz-Jacques, A. Leverrier, P. Grangier, and E. Diamanti, "Experimental demonstration of long-distance continuous-variable quantum key distribution," *Nat. Photon.*, vol. 7, no. 5, pp. 378–381, 2013.
[27] Y. Xia, W. Li, W. Clark, D. Hart, Q. Zhuang, and Z. Zhang, "Demonstration of a reconfigurable entangled radio-frequency photonic sensor network," *Phys. Rev. Lett.*, vol. 124, Apr. 2020, Art. no. 150502.
[28] N. Hosseinidehaj, Z. Babar, R. Malaney, S. X. Ng, and L. Hanzo, "Satellite-based continuous-variable quantum communications: State-of-the-art and a predictive outlook," *IEEE Commun. Surveys Tuts.*, vol. 21, no. 1, pp. 881–919, 1st Quart., 2019.
[29] C. W. Helstrom, "Detection theory and quantum mechanics," *Inf. Control*, vol. 10, no. 3, pp. 254–291, 1967.
[30] C. W. Helstrom, "Fundamental limitations on the detectability of electromagnetic signals," *Int. J. Theor. Phys.*, vol. 1, no. 1, pp. 37–50, May 1968.
[31] R. Yoshitani, "On the detectabillity limit of coherent optical signals in thermal radiation," *J. Stat. Phys.*, vol. 2, no. 4, pp. 347–378, Dec. 1970.
[32] M. Takeoka and M. Sasaki, "Discrimination of the binary coherent signal: Gaussian-operation limit and simple non-Gaussian near-optimal receivers," *Phys. Rev. A*, vol. 78, Aug. 2008, Art. no. 022320.
[33] N. Dalla Pozza and G. Pierobon, "Optimality of square-root measurements in quantum state discrimination," *Phys. Rev. A*, vol. 91, Apr. 2015, Art. no. 042334.
[34] R. Yuan, M. Zhao, S. Han, and J. Cheng, "Kennedy receiver using threshold detection and optimized displacement under thermal noise," *IEEE Commun. Lett.*, vol. 24, no. 6, pp. 1313–1317, Jun. 2020.
[35] R. J. Glauber, "The quantum theory of optical coherence," *Phys. Rev.*, vol. 130, pp. 2529–2539, Jun. 1963.
[36] R. J. Glauber, "Coherent and incoherent states of the radiation field," *Phys. Rev.*, vol. 131, pp. 2766–2788, Sep. 1963.
[37] K. E. Cahill and R. J. Glauber, "Ordered expansions in boson amplitude operators," *Phys. Rev.*, vol. 177, pp. 1857–1881, Jan. 1969.
[38] K. E. Cahill and R. J. Glauber, "Density operators and quasiprobability distributions," *Phys. Rev.*, vol. 177, pp. 1882–1902, Jan. 1969.
[39] R. E. Slusher and B. Yurke, "Squeezed light for coherent communications," *J. Lightw. Technol.*, vol. 8, no. 3, pp. 466–477, Mar. 1990.
[40] G. Cariolaro, R. Corvaja, and G. Pierobon, "Gaussian states and geometrically uniform symmetry," *Phys. Rev. A*, vol. 90, Oct. 2014, Art. no. 042309.
[41] G. Chesi, S. Olivares, and M. G. A. Paris, "Squeezing-enhanced phase-shift-keyed binary communication in noisy channels," *Phys. Rev. A*, vol. 97, Mar. 2018, Art. no. 32315.
[42] L. Mandel, "Ideal light source for an optical communication channel," *J. Opt. Soc. Amer.*, vol. 66, no. 9, pp. 968–970, Sep. 1976.
[43] C. M. Caves and P. D. Drummond, "Quantum limits on bosonic communication rates," *Rev. Mod. Phys.*, vol. 66, pp. 481–537, Apr. 1994.
[44] A. Vourdas, "Optical signals with thermal noise," *Phys. Rev. A*, vol. 39, pp. 206–213, Jan. 1989.
[45] G. S. Agarwal and K. Tara, "Nonclassical properties of states generated by the excitations on a coherent state," *Phys. Rev. A*, vol. 43, pp. 492–497, Jan. 1991.

[46] A. Zavatta, S. Viciani, and M. Bellini, "Quantum-to-classical transition with single-photon-added coherent states of light," *Science*, vol. 306, no. 5696, pp. 660–662, 2004.

[47] A. Zavatta, S. Viciani, and M. Bellini, "Single-photon excitation of a coherent state: Catching the elementary step of stimulated light emission," *Phys. Rev. A*, vol. 72, Aug. 2005, Art. no. 023820.

[48] S. Guerrini, M. Chiani, M. Z. Win, and A. Conti, "Quantum pulse position modulation with photon-added coherent states," in *Proc. IEEE Workshop Quantum Commun. Inf. Technol. (QCIT) Global Telecommun. Conf.*, Waikoloa, HI, USA, Dec. 2019, pp. 1–5.

[49] D. Wang *et al.*, "Quantum key distribution with the single-photon-added coherent source," *Phys. Rev. A*, vol. 90, Dec. 2014, Art. no. 062315.

[50] R. Zhang, X.-G. Meng, C.-X. Du, and J.-S. Wang, "Nonclassicality of photon-added displaced thermal state via quantum phase-space distributions," *J. Phys. Soc. Jpn.*, vol. 87, no. 2, 2018, Art. no. 024001.

[51] X.-X. Xu, L.-Y. Hu, and H.-Y. Fan, "Photon-added squeezed thermal states: Statistical properties and its decoherence in a photon-loss channel," *Opt. Commun.*, vol. 283, no. 9, pp. 1801–1809, 2010.

[52] S. Wang and H.-Y. Fan, "Phase-sensitive nonclassical properties of photon-added displaced squeezed thermal states," *J. Opt. Soc. Amer. B*, vol. 29, no. 7, pp. 1672–1679, Jul. 2012.

[53] M. M. Wilde, *Quantum Information Theory*, 2nd ed. Cambridge, U.K.: Cambridge University Press, 2017.

[54] M. Abramowitz and I. A. Stegun, *Handbook of Mathematical Functions*. New York, NY, USA: Dover Publications, 1970.

[55] C. W. Gardiner and P. Zoller, *Quantum Noise*, 3rd ed. Berlin, Germany: Springer, 2004.

[56] A. Zavatta, V. Parigi, and M. Bellini, "Experimental nonclassicality of single-photon-added thermal light states," *Phys. Rev. A*, vol. 75, May 2007, Art. no. 052106.

[57] A. Kenfack and K. Zyczkowski, "Negativity of the Wigner function as an indicator of non-classicality," *J. Opt. B: Quantum Semiclass. Opt.*, vol. 6, no. 10, pp. 396–404, Aug. 2004.

[58] G. S. Agarwal and K. Tara, "Nonclassical character of states exhibiting no squeezing or sub-Poissonian statistics," *Phys. Rev. A*, vol. 46, pp. 485–488, Jul. 1992.

[59] H. Yuen and J. Shapiro, "Optical communication with two-photon coherent states–part III: Quantum measurements realizable with photoemissive detectors," *IEEE Trans. Inf. Theory*, vol. 26, no. 1, pp. 78–92, Jan. 1980.

[60] H. Yuen and J. Shapiro, "Optical communication with two-photon coherent states–part I: Quantum-state propagation and quantum-noise," *IEEE Trans. Inf. Theory*, vol. 24, no. 6, pp. 657–668, Nov. 1978.

[61] B. R. Mollow and R. J. Glauber, "Quantum theory of parametric amplification. I," *Phys. Rev.*, vol. 160, pp. 1076–1096, Aug. 1967.

[62] R. R. Puri, *Mathematical Methods of Quantum Optics*. Berlin, Germany: Springer, 2001.

[63] M. Kracht and E. Kreyszig, *Methods of Complex Analysis in Partial Differential Equations with Applications*. New York, NY, USA: Wiley, 1988.

[64] C. L. Mehta, "Diagonal coherent-state representation of quantum operators," *Phys. Rev. Lett.*, vol. 18, pp. 752–754, May 1967.

[65] W. P. Schleich, *Quantum Optics in Phase Space*. Berlin, Germany: Wiley, 2001.

[66] U. Leonhardt, *Measuring The Quantum State of Light*. Cambridge, U.K.: Cambridge University Press, 1997.

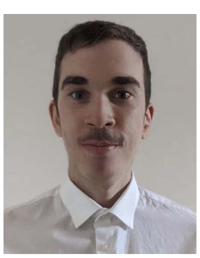

Stefano Guerrini (Student Member, IEEE) received the Laurea degree (*summa cum laude*) in electronics and telecommunications engineering in 2017 from the University of Ferrara, where he is currently pursuing a Ph.D. degree.

Since 2017, he has been a research assistant in the Wireless Communication and Localization Networks Laboratory at the University of Ferrara. In Spring 2020, he visited the Wireless Information and Network Sciences Laboratory at the Massachusetts Institute of Technology. His current research topics include statistical inference and quantum information science.

Mr. Guerrini served as a reviewer for different IEEE journals and international conferences.

Moe Z. Win (Fellow, IEEE) is a Professor at the Massachusetts Institute of Technology (MIT) and founding director of the Wireless Information and Network Sciences Laboratory. Prior to joining MIT, he was with AT&T Research Laboratories and with NASA Jet Propulsion Laboratory.

His research encompasses fundamental theories, algorithm design, and network experimentation for a broad range of real-world problems. His current research topics include network localization and navigation, network interference exploitation, and quantum information science. He has served the IEEE Communications Society as an elected Member-at-Large on the Board of Governors, as elected Chair of the Radio Communications Committee, and as an IEEE Distinguished Lecturer. Over the last two decades, he held various editorial positions for IEEE journals and organized numerous international conferences. Recently, he has served on the SIAM Diversity Advisory Committee.

Dr. Win is an elected Fellow of the AAAS, the EURASIP, the IEEE, and the IET. He was honored with two IEEE Technical Field Awards: the IEEE Kiyo Tomiyasu Award (2011) and the IEEE Eric E. Sumner Award (2006). His publications, co-authored with students and colleagues, have received several awards. Other recognitions include the IEEE Communications Society Edwin H. Armstrong Achievement Award (2016), the Cristoforo Colombo International Prize for Communications (2013), the Copernicus Fellowship (2011) and the *Laurea Honoris Causa* (2008) from the Università degli Studi di Ferrara, and the U.S. Presidential Early Career Award for Scientists and Engineers (2004). He is an ISI Highly Cited Researcher.

Marco Chiani (Fellow, IEEE) received the Dr. Ing. degree (*summa cum laude*) in electronic engineering and the Ph.D. degree in electronic and computer engineering from the University of Bologna, Italy, in 1989 and 1993, respectively.

He is a Full Professor of Telecommunications at the University of Bologna. During Summer 2001, he was a Visiting Scientist at AT&T Research Laboratories, Middletown, NJ. Since 2003 he has been a frequent visitor at the Massachusetts Institute of Technology (MIT), Cambridge, where he presently holds a Research Affiliate appointment. His research interests are in the areas of communications theory, wireless systems, coding theory, and statistical signal processing. In 2012 he has been appointed Distinguished Visiting Fellow of the Royal Academy of Engineering, UK. He served as elected Chair (2002–2004) of the Radio Communications Committee of the IEEE Communication Society and as Editor (2000–2007) of Wireless Communication for the IEEE TRANSACTIONS ON COMMUNICATIONS.

He received the 2011 IEEE Communications Society Leonard G. Abraham Prize in the Field of Communications Systems, the 2012 IEEE Communications Society Fred W. Ellersick Prize, and the 2012 IEEE Communications Society Stephen O. Rice Prize in the Field of Communications Theory.

Andrea Conti (Senior Member, IEEE) is a Professor and founding director of the Wireless Communication and Localization Networks Laboratory at the University of Ferrara, Italy. Prior to joining the University of Ferrara, he was with CNIT and with IEIIT-CNR.

In Summer 2001, he was with the Wireless Systems Research Department at AT&T Research Laboratories. Since 2003, he has been a frequent visitor to the Wireless Information and Network Sciences Laboratory at the Massachusetts Institute of Technology, where he presently holds the Research Affiliate appointment. His research interests involve theory and experimentation of wireless communication and localization systems. His current research topics include network localization and navigation, distributed sensing, adaptive diversity communications, and quantum information science.

Dr. Conti has served as editor for IEEE journals and chaired international conferences. He was elected Chair of the IEEE Communications Society's Radio Communications Technical Committee and is Co-founder of the IEEE Quantum Communications & Information Technology Emerging Technical Subcommittee. He received the HTE Puskás Tivadar Medal, the IEEE Communications Society's Fred W. Ellersick Prize, and the IEEE Communications Society's Stephen O. Rice Prize in the field of Communications Theory. He is an elected Fellow of the IET and a member of Sigma Xi. He has been selected as an IEEE Distinguished Lecturer.